Journal of the Korean Physical Society, Vol. 45, No. 1, July 2004, pp. 1∼5

Influence of Ion Irradiation on the Magnetic Properties of Fe/Cr Multilayers

F. Stobiecki,* B. Szymański, M. Urbaniak, T. Luciński and J. Dubowik
Institute of Molecular Physics, Polish Academy of Sciences, Poznań, Poland

M. Kopcewicz and J. Jagielski
Institute of Electronic Materials Technology, Warsaw, Poland

Y. P. Lee†
Quantum Photonic Science Research Center and Department of Physics, Hanyang University, Seoul 133-791

(Received 28 November 2003)

The influence of Ar-ion irradiation on the microstructure and magnetic properties of Fe/Cr multilayers is studied. An increase in the interface roughness of Fe/Cr multilayers, caused by irradiation with 200 keV Ar ions whose dose exceeds 5×10^{12} Ar/cm^2, is clearly seen by conversion electron Mössbauer spectroscopy (CEMS). This modification of the microstructure induces distinct changes in the magnetization reversal (an increase in remanence magnetization and a decrease in saturation field), and greatly reduces the giant magnetoresistance (GMR) effect on increasing the irradiation dose. An enhanced immunity of the GMR effect to the ion irradiation on increasing the thickness of Cr layers, as well as correlation between the changes of GMR and the antiferromagnetically coupled fraction, suggests that the main effect responsible for the decrease in GMR is the formation of pinholes. The temperature dependence of remanence magnetization confirms increases in pinhole density and size during implantation. However, for doses exceeding 2×10^{13} Ar/cm^2, volume intermixing seems to be a dominant mechanism responsible for the further degradation of GMR and the antiferromagnetic interlayer exchange coupling.

PACS numbers: 68.35.-p, 75.47.De, 75.70.Cn, 76.80.+y
Keywords: Fe/Cr multilayer, Magnetic properties, Ion irradiation

I. INTRODUCTION

Antiferromagnetic interlayer exchange coupling [1, 2] and the giant magnetoresistance (GMR) effect were discovered in Fe/Cr multilayers more than fifteen years ago, and the theoretical description of this phenomenon is now well established [3]. Presently, magnetic multilayers with a strong antiferromagnetic interlayer exchange coupling form a new class of thin-film structures which can be employed as artificial antiferromagnets. These films are of interest, because of possible applications to GMR structures, instead of the conventional antiferromagnet [4], or to new magnetic storage media [5]. In thin-film technologies, thermal annealing and ion irradiation are the supplementary post-deposition treatments enabling a modification of the microstructure and, consequently, the magnetic properties. Furthermore, lateral resolution can easily be realized with ion irradiation [6]. Therefore, a correlation between changes in the microstructure, induced by irradiation, and the interlayer coupling and the GMR effect of multilayers seems to be of interest. Recently, it was shown that ion irradiation may lead either to an enhanced GMR effect or to degradation, depending on the ion dose. Irradiation with 500 keV Xe ions [7, 8] induced an initial increase in the GMR. However, at higher ion doses the GMR was destroyed. Irradiation with 200 MeV Ag-ions led to a reduced GMR effect in Fe/Cr multilayers [9]. Epitaxial Fe/Cr/Fe(001) trilayers with a thin Cr spacer ($t_{\mathrm{Cr}} \leq 0.7$ nm), irradiated with 5 keV He ions, showed a monotonic decrease in the antiferromagnetic coupling strength $|J_{\mathrm{AF}}|$ on increasing the ion dose [6]. However, for $t_{\mathrm{Cr}} \geq 0.7$ nm, $|J_{\mathrm{AF}}|$ initially slightly increases and then decreases. An enhanced immunity of the GMR and the antiferromagnetic coupling to ion irradiation for thicker Cr layers was also observed in our previous paper [10], and suggests that the main effect responsible for degraded GMR is pinhole formation upon irradiation.

In this contribution, the preliminary experimental results presented in [10] are supplemented by new ones. In particular, our investigations are extended to a new set of Fe/Cr multilayers with various thicknesses of Cr spacer, and to a wider range of Ar-ion dose.

*E-mail: stfeliks@ifmpan.poznan.pl
†E-mail: yplee@hanyang.ac.kr

II. EXPERIMENT

A Fe-3nm/Cr-1.1nm multilayer and a set of Fe-1.4 nm/Cr-$t_{\rm Cr}$ multilayers with different Cr layer thicknesses ($0.97 \leq t_{\rm Cr} \leq 1.85$ nm) were deposited on $\rm SiO_x$ substrates by using UHV magnetron sputtering (dc and rf for Fe and Cr, respectively). The deposition rate (0.04 nm/s for both materials) was monitored *in situ* with a quartz sensor. Additionally, the modulation wavelengths ($\lambda = t_{\rm Fe} + t_{\rm Cr}$) and the thicknesses of iron and chromium layers were *ex situ* controlled by small-angle X-ray diffraction (SAXRD) and X-ray fluorescence (XRF), respectively. The total thickness of the Fe/Cr films was about 100 nm. The samples were irradiated at room temperature (RT) with 200 keV Ar ions at doses $D_{\rm Ar}$ ranging from 5×10^{12} to 2×10^{14} Ar/cm^2. For the applied ion energy, the penetration depth is higher than the total thickness of the samples. The as-deposited and irradiated samples were characterized at RT by conversion electron Mössbauer spectroscopy (CEMS), SAXRD and VSM. Magnetoresistance and resistivity were measured by using the four-probe technique with current in-plane (CIP) geometry at RT. The $GMR(H)$ dependencies were determined as $GMR(H) = 100 \times [R(H) - R(H{=}2{\rm T})]/R(H{=}2{\rm T})$ (where H is the magnetic field); the maximal value of $GMR(H)$ is defined as the GMR amplitude. The temperature dependence of remanence magnetization was determined from hysteresis loops taken at temperatures ranging from 230 to 470 K.

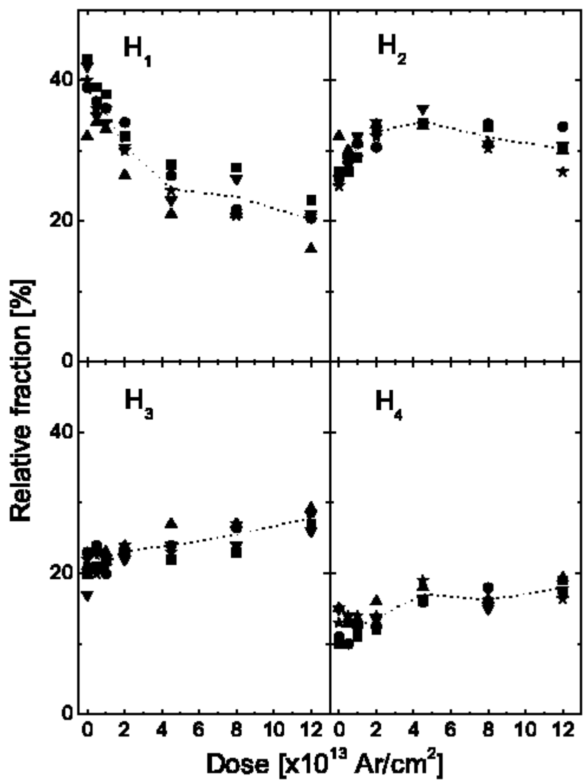

Fig. 1. Relative spectral fractions of H_1 – H_4 components vs ion dose for Fe-1.4 nm/Cr-$t_{\rm Cr}$ multilayers with $t_{\rm Cr}$ = 0.97 nm (■), $t_{\rm Cr}$ = 1.03 nm (●), $t_{\rm Cr}$ = 1.4 nm (▲), $t_{\rm Cr}$ = 1.5 nm (▼) and $t_{\rm Cr}$ = 1.85 nm (★). The lines are guides to the eye.

III. RESULTS AND DISCUSSION

The CEMS spectra for as-deposited and irradiated samples were fitted according to a model proposed by Landes *et al.* [11, 12]. In the model, four individual magnetic components with different values of hyperfine field H are associated with different iron environments: $H_1 \approx 33$ T corresponds to the bulk Fe sites; ($H_2 \approx 30$ T and $H_3 \approx 24$ T) contribute to the "step" sites at the Fe/Cr interfaces; $H_4 \approx 20$ T corresponds either to the "perfect" interface sites or to some other "step" positions. Such an analysis of CEMS spectra is helpful in investigations of microstructure changes of Fe/Cr multilayers during irradiation.

Figure 1 presents changes in the relative fraction of a particular component of CEMS spectra versus $D_{\rm Ar}$ for the set of Fe-1.4 nm/Cr-$t_{\rm Cr}$ multilayers. For samples characterized by ideally smooth interfaces, the expected relative fraction of H_1, H_4 components should be 71 % and 29 % (for $t_{\rm Fe} = 1.4$ nm ≈ 7 ML: the relative fraction of H_1 component is $5/7 = 71$ % and the relative fraction of H_4 component is $2/7 = 29$ %), respectively, and the contributions corresponding to H_2 and H_3 components should be zero [13]. In fact, even for the as-deposited samples, the measured fractions of H_1 and H_4 components are significantly smaller and H_2, H_3 fractions show nonzero values (see Figure 1, data for $D_{\rm Ar} = 0$). A value of relative fraction of H_1 component of about 40 % indicates that only 0.6 nm of each Fe layer corresponds to bulk Fe sites. The thickness of 0.6 nm (≈ 3 ML) is 2 ML thinner than those corresponding to Fe-1.4 nm/Cr-$t_{\rm Cr}$ structure with ideally smooth interfaces. Other Fe atoms, together with Cr atoms, form the interface regions corresponding to H_2, H_3 and H_4 components.

It should be noted that for multilayers with $t_{\rm Cr} \geq 1.4$ nm, apart from the ferromagnetic components, there is also a weak paramagnetic component (not included in Figure 1) related to isolated Fe atoms in Cr layers. The intensity of this component increases almost linearly with $D_{\rm Ar}$ (*e.g.* for Fe-1.4 nm/Cr-1.85 nm multilayer an increase of about 3 to 8 % is observed for the samples before and after irradiation with $D_{\rm Ar} = 1.2 \times 10^{14}$ Ar/cm^2, respectively). For multilayers with a thinner Cr layer, the amount of isolated Fe atoms (probably proportional to $t_{\rm Cr}$) was too small to be detected in CEMS spectra. The experimental value of the relative fraction of H_1 component determined for Fe-3nm/Cr-1.1nm multilayers is 73 % and indicates that only 2.2 nm ($\approx$ 11 ML instead 13 ML expected for smooth inter-

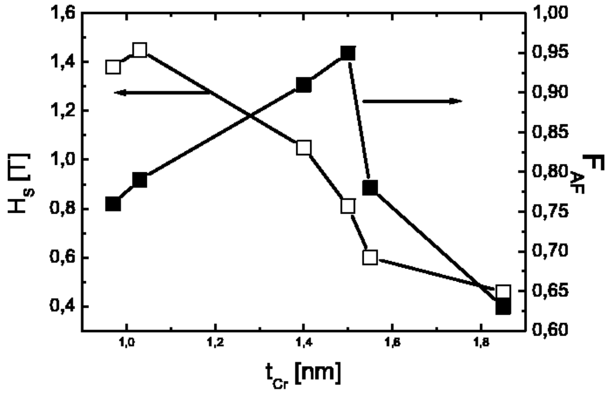

Fig. 2. Saturation field (H_S) and antiferromagnetically coupled volume fraction (F_{AF}) of as-deposited Fe-1.4 nm/Cr-t_{Cr} multilayers with different thickness of Cr spacer.

faces) corresponds to iron atoms in bulk positions. The similarity of this result to those obtained for films with $t_{Fe} = 1.4$ nm and $0.97 \text{ nm} \leq t_{Cr} \leq 1.85$ nm indicates that the interface structure of the as-deposited Fe/Cr multilayers is independent of the Fe and Cr layer thicknesses.

For multilayers with similar roughness of interfaces, the probability of formation of the magnetic bridges (pinholes) across the Cr spacer increases with reduced thickness [14]. The pinholes in the antiferromagnetically (AF) coupled multilayers lead to a strong ferromagnetic coupling localized in their vicinity [14–16]. As a result, the antiferromagnetically coupled fraction, F_{AF} (defined as $F_{AF} = 1 – M_R/M_S$, where M_R and M_S are the remanence and saturation magnetization determined from hysteresis loops) is less than one. Such a behavior is observed in our as-deposited samples. Nearly perfect antiferromagnetic coupling ($F_{AF} \approx 1$) was found for $t_{Cr} = 1.5$ nm (Figure 2). For smaller t_{Cr} the F_{AF} factor decreases, despite the growth in the antiferromagnetic coupling strengths (determined from the increase in saturation field), and indicates an increasing role of the direct coupling through the pinholes.

The significant changes in CEMS spectra corresponding to microstructure modification of Fe/Cr multilayers caused by Ar ion irradiation have already been detected at ion fluence $D_{Ar} \geq 5 \times 10^{12}$ Ar/cm^2. Nearly the same increase in the spectral contribution of the H_2 component, accompanied by a decrease in H_1 component, is observed for all Fe-1.4 nm/Cr-t_{Cr} multilayers (Figure 1). This suggests that the interface roughness (the number of Fe in the step sites) increases with increasing D_{Ar}, independently of t_{Cr}. The changes in the relative fraction of H_1-H_4 components with D_{Ar} determined for Fe-3nm/Cr-1.1nm structure [10] indicate a similar modification of the interface structures. However, in the SAXRD spectra no changes caused by the ion irradiation have been detected for $D_{Ar} \leq 5 \times 10^{13}$ Ar/cm^2. The poor sensitivity of the SAXRD method seems to be obvious on taking into account the small contrast between Fe and Cr in their refractive indices. Simultaneously with the subtle changes of CEMS spectra (Figure 1), distinct changes in magnetization reversal and magnetoresistance curves are observed for Fe/Cr multilayers with thin ($t_{Cr} < 1.4$ nm) spacer layers (Figure 3(a), (b)). All the features characteristic of the increasing density of pinholes [15], *i.e.*, the increase in M_R and the decrease in H_S, as well as the gradual disappearance of the linearity of $M(H)$ dependence (an increase of the biquadratic component of interlayer exchange coupling), can be recognized in the hysteresis loops measured after the successive steps of irradiation. Obviously, due to the correlation between $M(H)$ and $GMR(H)$ dependencies (see *e.g.* [17]), all the above mentioned changes in magnetic properties are also manifested in the $GMR(H)$ dependencies (Figure 3). For a multilayer with $t_{Fe} = t_{Cr} = 1.4$ nm (Figure 3(c), (d)), the influence of irradiation is quantitatively similar. However, the modifications of the particular parameters (F_{AF}, H_S, GMR) at $D_{Ar} \leq 2 \times 10^{13}$ Ar/cm^2 are significantly smaller than for the samples discussed above. An enhanced immunity of the F_{AF} parameter and GMR amplitude degradations to the ion irradiation with $D_{Ar} \leq 2 \times 10^{13}$ Ar/cm^2 is more distinct for multilayers with $t_{Cr} > t_{Fe}$ (see Figure 3(e), (f)). However, for the multilayers with $t_{Cr} \geq 1.4$ nm and $D_{Ar} \geq 4.5 \times 10^{13}$ Ar/cm^2 a distinct decrease in the GMR effect is accompanied by negligible changes in the shape of the hysteresis loops.

For multilayers with a similar thickness of Cr layers and different t_{Fe}, the changes in magnetic properties caused by the ion irradiation are similar (see Figure 4 for the magnetoresistance data). However, because $H_S \propto 1/t_{Fe}$, the corresponding saturation fields of the as-deposited and irradiated samples with $t_{Fe} = 1.4$ nm are about twice as large as those for multilayers with $t_{Fe} = 3$ nm. The difference in the magnetoresistance values is also obvious due to the crucial role of interface scattering in the GMR effect of Fe/Cr multilayers.

To summarize the study concerning the influence of the Ar-ion irradiation process on the magnetic properties of Fe/Cr multilayers with different Cr layer thicknesses, the dependencies of H_S, GMR and F_{AF} versus t_{Cr} are shown in Figure 5 for the as-deposited samples and after the successive steps of the irradiation process. The room-temperature $H_S(t_{Cr})$ and $GMR(t_{Cr})$ dependencies of the as-deposited samples are related to the oscillatory behavior of the interlayer exchange coupling with the local maximum at $t_{Cr} \approx 1.1$ nm, and are similar to those observed for the other sputtered Fe/Cr multilayers (see *e.g.* [18]). As we have stated above, for multilayers with a similar interface roughness the maximum of the $F_{AF}(t_{Cr})$ dependence is observed for the higher Cr layer thickness ($t_{Cr} \approx 1.5$ nm). The strong degradation of the antiferromagnetic coupling (decrease of H_S, GMR, F_{AF} with D_{Ar}) for low doses of irradiated ions ($D_{Ar} \leq 2 \times 10^{13}$ Ar/cm^2) is observed only for samples with a small thickness of the spacer layers ($t_{Cr} \leq 1.4$ nm). Such a behavior can be explained as

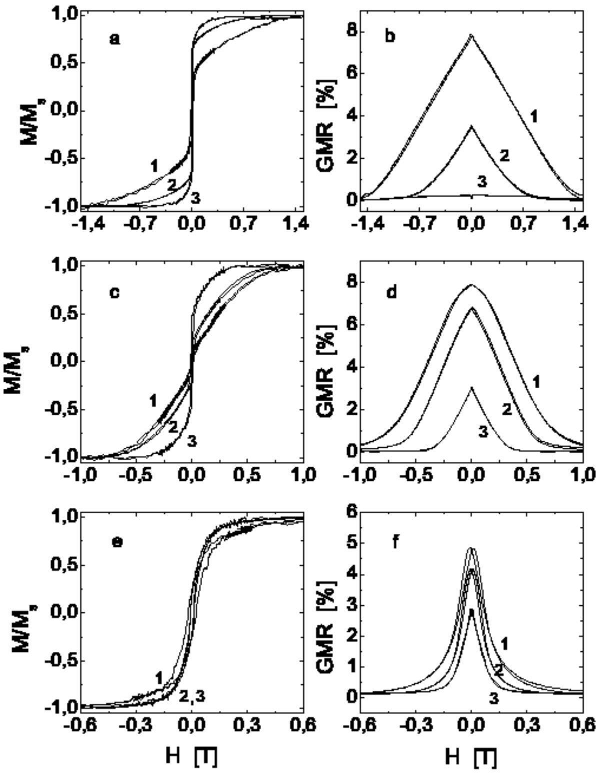

Fig. 3. Examples of hysteresis loops and $GMR(H)$ dependencies for as-deposited and irradiated Fe-1.4 nm/Cr-t_{Cr} samples, with (a), (b) t_{Cr} = 0.97 nm, (c), (d) t_{Cr} = 1.4 nm and (e), (f) t_{Cr} = 1.55 nm. Curves 1, 2 and 3 denote samples in the as-deposited state and irradiated with doses of 2×10^{13} Ar/cm^2 and 8×10^{13} Ar/cm^2, respectively.

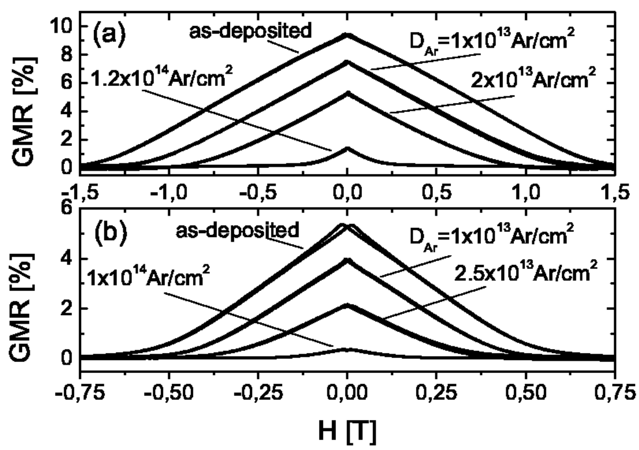

Fig. 4. $GMR(H)$ dependencies of (a) Fe-1.4 nm/Cr-1.03 nm and (b) Fe-3 nm/Cr-1.1 nm multilayers in the as-deposited state and after successive irradiation steps.

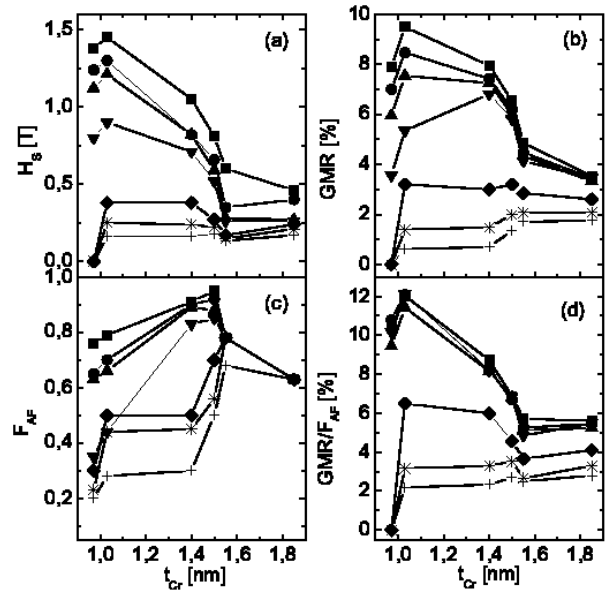

Fig. 5. Dependencies of saturation field H_S, GMR amplitude, antiferromagnetically coupled fraction F_{AF} and GMR/F_{AF} of Fe-1.4 nm/Cr-t_{Cr} multilayers as a function of t_{Cr} for as-deposited samples (■) and after successive irradiation with doses of 5×10^{12} Ar/cm^2 (●); 1×10^{13} Ar/cm^2 (▲); 2×10^{13} Ar/cm^2 (▼); 8×10^{13} Ar/cm^2 (♦); 1.2×10^{14} Ar/cm^2 (∗); 2×10^{14} Ar/cm^2 (+).

follows. As a result of the irradiation, the uncorrelated interface roughness increases independently of t_{Cr} (see discussion of Figure 1). Therefore, the probability of pinhole creation resulting in a decrease in F_{AF} is larger for multilayers with smaller t_{Cr}. Moreover, the proportionality between the GMR amplitude and F_{AF} should be observed, provided that only the antiferromagnetically coupled regions contribute to the GMR effect, for antiferromagnetically coupled multilayers with a different density of pinholes. Such a behavior, *i.e.*, negligible changes in the ratio GMR/F_{AF} with D_{Ar}, are also observed for our Fe/Cr multilayers within a whole range of t_{Cr} and for ion doses smaller than 2×10^{13} Ar/cm^2 (Figure 5(d)). This additionally supports our interpretation and indicates that the formation of pinholes is the main source of degradation of the antiferromagnetic coupling and the GMR effect. However, the loss of the correlation between F_{AF} and GMR amplitude, observed for the higher doses, indicates that another mechanism responsible for the decrease in the GMR with D_{Ar} starts to dominate at $D_{Ar} > 2 \times 10^{13}$ Ar/cm^2. The higher irradiation doses D_{Ar} result in the growth of the paramagnetic component, seen in CEMS, and in an increase in the electrical resistance [10], due to enhanced alloying, apart from growth in interface roughness. Due to an increasing number of defects in the multilayer structure, the mean free path of the electrons decreases, thus reducing the GMR effect. Moreover, with degradation of the structural order of the spacer layers, the strength of the antiferromagnetic coupling decreases and its oscillatory behavior gradually vanishes (Figure 5).

Despite the fact that the formation of the pinholes during the ion irradiation seems to be well documented in the above described results, we performed an addi-

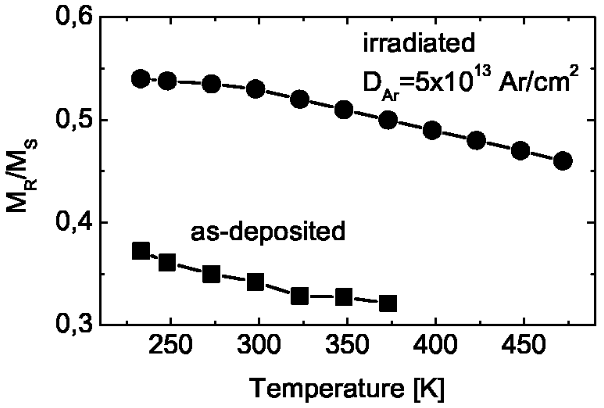

Fig. 6. Normalized remanence magnetization as a function of temperature for Fe-3 nm/Cr-1.1 nm multilayers in the as-deposited state and for samples irradiated with 5×10^{13} Ar/cm^2.

tional experiment, which confirms this finding. Due to the small cross-sectional area of pinholes, the size effects, typical of low dimensional magnetic entities, become important, leading to a strong reduction of the local ferromagnetic coupling via the thermal fluctuations of magnetic moments. As a consequence, with an enhanced density of pinholes and a growth of their cross-sectional area, both the low-temperature value of M_R and the temperature at which ferromagnetic coupling vanishes increase [15]. Such a characteristic behaviour can be seen in Figure 6 for the Fe-3nm/Cr-1.1nm multilayers, indicating that the main cause responsible for the degradation of F_{AF} and the GMR effect is related to the increase in pinhole density and their size during ion irradiation.

IV. CONCLUSIONS

Irradiation with 200 keV Ar ions was used as a post-preparation treatment of polycrystalline Fe/Cr multilayers with different layer thicknesses. The independence of Cr layer thickness with respect to interfacial roughness was deduced from CEMS measurements for doses exceeding 5×10^{12} Ar/cm^2. This results in a significantly stronger growth of pinhole density in the multilayers with thin Cr spacer layers. In consequence, a stronger degradation in the GMR effect and the antiferromagnetic interlayer exchange coupling with increasing irradiation dose is observed in the case of thin Cr layers. The correlation between changes in the GMR and the antiferromagnetically coupled fraction, as well as characteristic changes in the temperature dependence of remanence magnetization, additionally confirm the formation of pinholes during the ion irradiation. For the heavily irradiated Fe/Cr multilayers with doses exceeding 2×10^{13} Ar/cm^2, volume intermixing is the dominant mechanism responsible for degradation of the GMR and the antiferromagnetic coupling.

ACKNOWLEDGMENTS

This work was partially supported by KOSEF through the Quantum Photonic Science Research Center (q-Psi).

REFERENCES

[1] P. Grünberg, R. Schreiber, Y. Pang, M. B. Brodsky and H. Sowers, Phys. Rev. Lett. **57**, 2442 (1986).

[2] M. N. Baibich, J. M. Broto, A. Fert, F. Nguyen Van Dau, F. Petroff, P. Etienne, G. Creuzet, A. Friederych and J. Chazelas, Phys. Rev. Lett. **61**, 2472 (1988).

[3] R. E. Camley and J. Barnaś, Phys. Rev. Lett. **63**, 664 (1989); see also J. Barnaś, A. Fuss, R. E. Camley, P. Grünberg and W. Zinn, Phys. Rev. B **42**, 8110 (1990).

[4] J. Schmalhorst, H. Brückl, G. Reiss, R. Kinder, G. Gieres and J. Wecker, Appl. Phys. Lett. **77**, 3456 (2000).

[5] E. E. Fullerton, D. T. Margulies, M. E. Schabes, M. Carey, B. Gurney, A. Moser, M. Best, G. Zeltzer, K. Rubin and H. Rosen, Appl. Phys. Lett. **77**, 3806 (2000).

[6] S. O. Demokritov, C. Bayer, S. Poppe, M. Rickart, J. Fassbender, B. Hillebrands, D. I. Kholin, N. M. Kreines and O. M. Liedke, Phys. Rev. B **90**, 097201 (2003).

[7] D. M. Kelly, I. K. Schuller, V. Korenivski, K. V. Rao, K. K. Larsen, J. Bøttiger, E. M. Gyorgy and R. B. van Dover, Phys. Rev. B **50**, 3481 (1994).

[8] V. Korenivski, K. V. Rao, D. M. Kelly, I. K. Schuller, K. K. Larsen and J. Bøttiger, J. Magn. Magn. Mater. **140-144**, 549 (1995).

[9] A. Paul, A. Gupta, S. M. Chaudhari and D. M. Phase, Vacuum **60**, 401 (2001).

[10] M. Kopcewicz, F. Stobiecki, J. Jagielski, B. Szymański, M. Schmidt, J. Dubowik and J. Kalinowska, J. Appl. Phys. **93**, 5514 (2003).

[11] J. Landes, Ch. Sauer, R. A. Brand, W. Zinn, S. Mantl and Zs. Kajcsos, J. Magn. Magn. Mater. **86**, 71 (1990).

[12] F. Klinkhammer, Ch. Sauer, E. Yu. Tsymbal, S. Handschuh, Q. Leng and W. Zinn, J. Magn. Magn. Mater. **161**, 49 (1996).

[13] N. M. Rensing, B. M. Clemens and D. L. Williamson, J. Appl. Phys. **79**, 7757 (1996).

[14] J. F. Bobo, M. Piecuch and E. Snoeck, J. Magn. Magn. Mater. **126**, 440 (1993).

[15] D. B. Fulghum and R. E. Camley, Phys. Rev. B **52**, 13436 (1995).

[16] J. F. Bobo, H. Kikuchi, O. Redon, E. Senoeck, M. Piecuch and R. L. White, Phys. Rev. B. **60**, 4131 (1999).

[17] B. Rodomacq, K. Dumesnil, P. Mangin and M. Hennion, Phys. Rev. B. **48**, 3556 (1993).

[18] M. A. M. Gijs and M. Okada, J. Magn. Magn. Mater. **113**, 105 (1992).